Int J Adv Manuf Technol (2015) 81:1303–1317
DOI 10.1007/s00170-015-7266-0

ORIGINAL ARTICLE

Optimization of process parameters on surface integrity in wire electrical discharge machining of tungsten tool YG15

Zhen Zhang[1,3] · Wuyi Ming[2] · Hao Huang[1] · Zhi Chen[1] · Zhong Xu[1] · Yu Huang[1] · Guojun Zhang[1]

Received: 5 February 2015 / Accepted: 4 May 2015 / Published online: 20 May 2015

Abstract This study mainly investigates the effect and optimization of process parameters on surface integrity including white layer thickness and crack density in wire electrical discharge machining (WEDM) of tungsten tool YG15 which is one of the most important hardened stainless steel alloys used in the mold industries. In this paper, four input process parameters including pulse-on time, pulse current, water pressure, and feed rate were set during WEDM experiment, and three output characteristics including surface roughness (SR), white layer thickness (WLT), and surface crack density (SCD) were taken as the performance criteria of surface integrity. Then an experiment for central composite design (CCD) of processing the tungsten tool YG15 has been conducted according to response surface methodology (RSM). After analyzing the experimental results and optimizing the WEDM process using two different methods namely backpropagation neural network combined with genetic algorithm (BPNN-GA) and Non-dominated Sorting Genetic Algorithm-II (NSGA-II), the optimal solution can be obtained. The analysis results manifest that the pulse-on time and pulse current have a significant effect on the SR, WLT, and SCD. Moreover, several confirmation tests were carried out to verify the efficiency of the optimization methods, and then the more appropriate method was demonstrated by the comparison of optimization results. According to analysis and discussion of results, the most suitable process parameter combinations can be obtained to guide the actual machine, which contribute to increase the surface integrity and accuracy of WEDM and simultaneously reduce the ratio of disqualification for industrial application.

Keywords Optimization · WEDM · Tungsten tool YG15 · White layer thickness · Crack density

1 Introduction

Wire electrical discharge machining is one of the high precision processing equipment for difficult-to-machine materials such as tungsten tool YG15 and SKD11, which are widely used in the mold, instrument, and manufacturing industries. The WEDM process is a strong electro-thermal process with the extremely high temperature and massive electrical discharges in a fraction of a second, which results in the poor surface quality such as high tensile residual stresses, high surface roughness, white layers, and micro cracks. During machining, the remaining materials which cannot be removed by a dielectric circulation system would rapidly solidify to create a recast layer also known as the white layer. The heat affected zone (HAZ) is under the white layer. Meanwhile, this process generates the residual stress leading to lots of micro-cracks and pores on the surface of white layer and in the HAZ, which damage the surface integrity and even reduce the fatigue strength [1–3]. Therefore, to reduce the surface roughness, white layer and

✉ Hao Huang
huanghaohust1990@gmail.com

[1] State Key Laboratory of Digital Manufacturing Equipment & Technology, School of Mechanical Science and Engineering, Huazhong University of Science & Technology, Wuhan, China

[2] Department of Electromechanical Science and Engineering, Zhengzhou University of Light Industry, Zhengzhou, China

[3] Mechanical Science and Engineering, University of Illinois at Urbana-Champaign, Urbana, USA

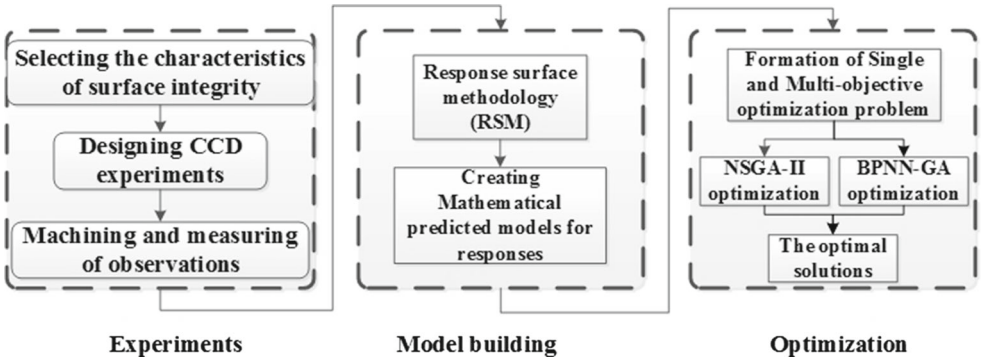

Fig. 1 Flow chart of overall optimization

micro-crack can develop the surface integrity of workpiece and enhance the mechanical properties, and the study of the effect of process parameters on the surface characteristics of WEDM surfaces including surface roughness (SR), white layer thickness (WLT) and surface crack density (SCD), and optimization of surface integrity is very necessary.

1.1 Literature review

In the WEDM process, surface integrity including the surface roughness, white layer, and micro cracks has a close relationship with the surface quality and mechanical properties of workpiece materials [1]. So investigation and optimization of process parameters on the surface characteristics are very crucial. Up to now, there are many researchers studying the surface integrity of workpiece materials in EDM or WEDM process.Because EDM process still has something different from WEDM process, Caydas and Hascalik [4] established a mathematic model of electrode wear (EW) and WLT through response surface methodology (RSM) in a die-sinking EDM, and they found that pulse current was the most significant factor influencing both the EW and WLT, while pulse-off time had little effect on both responses. Yildiz et al. [5] also developed an empirical model to predict the WLT during electro discharge drilling (EDD), a process similar to die-sinking EDM process. Pradhan [6] proposed a new hybrid method, using RSM coupled with the grey relational analysis, to estimate the effect of process parameters on surface integrity (including SR, WLT, and SCD) of EDM machining AISI D2 tool steel. Li and Tai [7] investigated the relationship between EDM parameters and surface crack formation using a full factorial design, based on pulse current and pulse-on time parameters. Puri and Bhattacharyya [8] have modeled the white layer depth through response surface methodology (RSM) in a WEDM process. They observed that the white layer depth increases with increasing pulse-on time during the first cut, while it decreases sharply with the increase of pulse-on time during trim cutting. It also dropped with reducing wire tool offset during trim cutting. Shahali et al. [9] applied micro-genetic algorithm and signal to noise ratio technique to optimize the SR and WLT of WEDM machining DIN1.4542 stainless steel and improve the surface quality of workpiece materials. Shabgard et al. [10] proposed an axisymmetric 3D model for temperature distribution in WEDM processing AISI H13 tool steel to estimate the WLT, HAZ, and SR using the finite element method and experimental investigation.

Although the researches on the effect of EDM process parameters on surface integrity characteristics including SR, WLT, HAZ, and SCD have been presented by some researchers, there are few studies about the effect of WEDM process parameters on surface integrity characteristics, especially including SR, WLT, and SCD at the same time, and the optimization of the process parameters to obtain a good surface integrity. In term of workpiece materials, though tungsten tool YG15 is one of the most important hardened stainless steel alloys used in the mold industries, there are few previous investigations on this material about surface integrity characteristics during WEDM process. Therefore, this paper mainly investigates the effect and optimization of process parameters on surface integrity including SR, WLT, and SCD in machining tungsten tool YG15 by WEDM.

1.2 Outline of the work

In this paper, according to our experience, literature survey and the characteristics of the experimental equipment, four process parameters, namely pulse-on time, pulse current,

Table 1 Physical properties of the YG15 steel

Properties	Value
Density (g/cm^3)	13.9
Hardness (HRA)	87˜90
Bending strength (N/mm^2)	2250
Average particle (nm)	1.5
Coefficient of expansion (°C^{-1})	5.3×10^{-6}

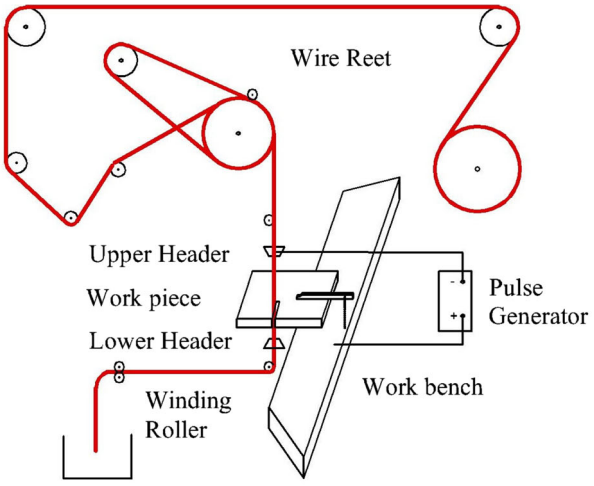

(a) Schematic drawing

(b) Photograph of the WEDM machine

(c) Photograph of specimens

Fig. 2 The experimental equipment and specimen

water pressure, and feed rate, are regarded as the input factors, while three response outputs are SR, WLT, and SCD. Then based on RSM, a four-factor, five-level experiment with 31 runs for central composite design (CCD) of processing the tungsten tool YG15 has been conducted. After the analysis of variance (ANOVA), the effect of process parameters on SR, WLT, and SCD can be concluded, and the mathematical regression models of SR, WLT, and SCD, respectively, are also established by RSM. Then, two different methods, namely BPNN-GA and NSGA-II (coded by using Matlab 2014a), are proposed to optimize the process parameters of WEDM for obtaining the optimal surface integrity with minimizing SR,WLT, and SCD, which is the main objective of this research. Moreover, these two approaches have proven their effectiveness because they have been successfully implemented to find out the optimal parameters on material removal rate (MRR) and 3D surface quality of WEDM [11–13] or to optimize the process of laser brazing [14]. Finally, the confirmation experiment is conducted to verify the efficiency of these methods applied in optimizing surface integrity characteristics. Meanwhile, the relationship between the process parameters and SR, WLT, and SCD can be also found out. The overall procedure of the present investigation is illustrated in Fig. 1.

2 Experimental setup and equipment

2.1 Materials

The workpiece is a 10-mm-thickness, 100-mm-length, 100-mm-wideth block of tungsten tool YG15 (wc: 85 %, co: 15 %) with the high hardness, which is suitable for manufacturing of the ramming mold, bearings, the abrasion spare part and so on. Table 1 shows the physical properties of the workpiece.

2.2 Equipment and specimens

The experiments are carried out by a high-performance, 5-axis computer numerically controlled (CNC) WEDM machine with anti-electrolysis plus generator in order to avoid oxidation of the workpiece. Figure 2 illustrates the schematic drawing and photograph of the experimental equipment. The wire tool is copper wire with a diameter of 0.25 mm. Then 5-mm-length through cuts are made on the test pieces according to the design of machining experiments on the WEDM. The other details of WEDM machine have been listed in Table 2.

2.3 Measurement of surface characteristics

In this paper, three vital characteristics of surface integrity including SR, WLT, and SCD would be studied. Root mean

Table 2 Fixed machining condition of WEDM

Parameters	Value
Material	Tungsten tool YG15
Shape and size of specimens (mm)	Rectangular, $10 \times 5 \times 5$
Angle of cut	Vertical
Dielectric temperature (°C)	25
Cutting speed	100 %

Table 3 Factors and their level for machining experiments

Factors	Symbol	Factor levels on machining experiments				
		1	2	3	4	5
Pulse-on time (μs):time of the discharge pulse duration of high level	A	5	7	9	11	13
Pulse current (A):	B	1	2	3	4	5
Water pressure (kg/cm^2):the impact pressure of dielectric flow.	C	1	4	7	10	13
Feedrate (mm/min):	D	0.3	0.45	0.6	0.75	0.9

square roughness (Rq) instead of average surface roughness (Ra) was used to profile the surface roughness (SR) due to the high accuracy of Rq describing the SR. The Rq was measured by Multi-functional Optical Aspheric Measurement System (Taylor Hobson PGI Dimension XL), which was set to a cutoff length of 0.8 mm, the traverse speed of 1 mm/s, and 5 mm evaluation length, for three times at three different locations in the same transverse direction. The final reported roughness Rq (in micrometers) of each sample was the average of these three measurements.

As for the measurement of WLT, the cross section of each specimen should be pre-processed. To analyze in both

Table 4 Experimental design and results by RSM

No.	A	B	C	D	SR(Rq)(μm)	WLT (μm)	SCD (μm/μm^2)
1	7	2	4	0.45	3.213	1.69	0.0288
2	11	2	4	0.45	1.460	1.64	0.0362
3	7	4	4	0.45	1.467	1.91	0.0325
4	11	4	4	0.45	2.777	5.39	0.1377
5	7	2	10	0.45	1.719	1.67	0.0602
6	11	2	10	0.45	1.790	1.75	0.0506
7	7	4	10	0.45	4.744	2.41	0.0444
8	11	4	10	0.45	3.854	3.08	0.0396
9	7	2	4	0.75	2.188	2.31	0.0598
10	11	2	4	0.75	2.324	1.75	0.0527
11	7	4	4	0.75	2.031	2.17	0.0532
12	11	4	4	0.75	1.974	4.86	0.1766
13	7	2	10	0.75	1.272	1.78	0.0860
14	11	2	10	0.75	1.516	1.92	0.0657
15	7	4	10	0.75	1.536	2.02	0.0554
16	11	4	10	0.75	1.203	2.37	0.0890
17	5	3	7	0.6	1.996	2.39	0.0780
18	13	3	7	0.6	1.706	1.27	0.0930
19	9	1	7	0.6	1.235	1.59	0.0518
20	9	5	7	0.6	1.629	2.98	0.0924
21	9	3	1	0.6	1.808	2.57	0.0485
22	9	3	13	0.6	2.825	1.67	0.0528
23	9	3	7	0.3	1.816	1.51	0.0468
24	9	3	7	0.9	1.156	1.44	0.0659
25	9	3	7	0.6	1.374	1.65	0.0618
26	9	3	7	0.6	1.390	1.64	0.0622
27	9	3	7	0.6	1.383	1.65	0.0634
28	9	3	7	0.6	1.378	1.66	0.0629
29	9	3	7	0.6	1.364	1.67	0.0612
30	9	3	7	0.6	1.369	1.63	0.0608

Table 5 Analysis of variance for SR(Rq)(μm)

Source	Sum of squares	df	Mean square	*F* value	*P* value	
Model	16.27	13	1.25	5.53	0.0009	Significant
A-A	0.14	1	0.14	0.63	0.4381	
B-B	1	1	1	4.4	0.0521	Significant
C-C	0.21	1	0.21	0.92	0.352	
D-D	2.87	1	2.87	12.67	0.0026	Significant
AB	0.11	1	0.11	0.49	0.4939	
AC	0.018	1	0.018	0.081	0.7797	
BC	2.23	1	2.23	9.86	0.0063	Significant
BD	1.7	1	1.7	7.51	0.0145	Significant
CD	2.39	1	2.39	10.54	0.0051	Significant
A^2	0.78	1	0.78	3.46	0.0812	
C^2	2.27	1	2.27	10.01	0.006	Significant
ABC	1.21	1	1.21	5.36	0.0342	Significant
BCD	1.6	1	1.6	7.07	0.0172	Significant
Residual	3.62	16	0.23			
Pure error	4.47E-04	5	8.95E-05			
Cor total	19.89	29				

the planar and cross-sectional views, the cross-section view was prepared in an epoxy mount and polished mechanically with silicon carbide paper with different grit sizes from small to large (120, 220, 320, 400, and 800), and this procedure lasted for 15 min. Moreover, the finish polishing was done with the diamond paste of 1-μm size. After mechanical polishing, the specimens were chemically etched by 20 % $K_3[Fe(CN)_6]$ and NaOH for 10 s, and then their surface were washed and cleaned by pure water. This procedure took rather long time till the white layer structure and the boundary line can be presented clearly. Finally, the specimens were observed by a thermal field emission scanning electron microscope (SEM) of JEOL JSM-7600F at $\times$1000 magnification. The WLT of each specimen was measured at nine locations on the cross-section, and the average value of the nine values was recorded.

Table 6 Analysis of variance for WLT(μm)

Source	Sum of squares	df	Mean square	*F* value	*P* value	
Model	22.36	12	1.86	13.02	<0.0001	Significant
A-A	0.63	1	0.63	4.38	0.0516	
B-B	6.49	1	6.49	45.41	<0.0001	Significant
C-C	1.77	1	1.77	12.4	0.0026	Significant
D-D	0.01	1	0.01	0.071	0.7926	Significant
AB	3.6	1	3.6	25.14	0.0001	Significant
AC	1.17	1	1.17	8.17	0.0109	Significant
BC	1.09	1	1.09	7.62	0.0134	Significant
A^2	0.41	1	0.41	2.89	0.1072	
B^2	1.55	1	1.55	10.84	0.0043	Significant
C^2	1.05	1	1.05	7.37	0.0147	Significant
ABC	2.23	1	2.23	15.6	0.001	Significant
AB^2	2.65	1	2.65	18.52	0.0005	Significant
Residual	2.43	17	0.14			
Pure error	1.00E-03	5	2.00E-04			
Cor total	24.79	29				

Table 7 Analysis of variance for SCD(μm/μm)

Source	Sum of squares	df	Mean square	*F* value	*P* value	
Model	0.024	9	2.67E-03	23.14	<0.0001	Significant
A-A	2.77E-03	1	2.77E-03	23.99	<0.0001	Significant
B-B	3.03E-03	1	3.03E-03	26.23	<0.0001	Significant
C-C	2.55E-04	1	2.55E-04	2.21	0.153	
D-D	2.53E-03	1	2.53E-03	21.91	0.0001	Significant
AB	5.15E-03	1	5.15E-03	44.6	<0.0001	Significant
AC	3.31E-03	1	3.31E-03	28.67	<0.0001	Significant
BC	4.11E-03	1	4.11E-03	35.64	<0.0001	Significant
A^2	1.08E-03	1	1.08E-03	9.38	0.0061	Significant
ABC	1.80E-03	1	1.80E-03	15.59	0.0008	Significant
Residual	2.31E-03	20	1.15E-04			
Pure error	4.92E-06	5	9.83E-07			
Cor total	0.026	29				

It is difficult to quantify the cracks due to an approximation of the width, length, or depth of the crack and the number of cracks, so a term, SCD, is defined as the total length of cracks µm in a unit area μm^2 to estimate the severity of cracking [7]. Though this definition was used in the EDM process, it can be extended to the WEDM process because of the similar principle of machining. The specimens were observed under SEM at ×3000 magnification, and the average crack length of each specimen, which is the total length of cracks selected randomly six-sample micrographs on each specimen, was divided by the number (six) of samples taken, was obtained. Then the SCD can be calculated by dividing the average crack lengths by the average area(1200 μm^2) of the sample micrographs.

2.4 Design of experiments and experimental results

An appropriate design of experiment can provide the optimal result with higher efficiency, accuracy in analysis at the minimum cost. Though RSM just requires a small number of runs and several levels of the independent variables, it is sufficient enough to offer much information and convey the majority of steady-state process responses [15]. For the sake of improving a mathematical model capacity of predicting the performance of the process under given input factors, a reasonable set of input parameters should be selected. According to our experience, literature survey, the characteristics of the experimental equipment, and some preliminary investigations, the surface integrity of WEDM is mainly affected by input parameters as follows:

1. A-pulse-on time
2. B-pulse current
3. C-water pressure
4. D-feedrate

Table 3 demonstrates the values and levels of the input parameters in the experiments, which cover the reasonable range of the input parameters available according to the characteristics of WEDM. Based on the RSM, a five-level, four-factor uniform-precision central composite rotatable factorial design (CCD) consisting of 30 runs of coded conditions for the modeling of the WEDM process is presented in Table 4. Design expert 8.0, which is a popular statistical analysis software, is used for designing CCD experiments and modeling the respond surface in this study.

3 Result analysis and discussion

The models of surface integrity characteristics of WEDM process can be simplified as a problem to correlate the input variables with their response. RSM technique is a useful method to handle this problem, and more details about RSM can be learned from references [11, 15].

3.1 Mathematical predicted models

Three mathematical predictive models of SR, WLT, and SCD were developed, respectively, by the RSM due to the high prediction accuracy of this model, which can be employed in prediction and optimization. The adequacy of each mathematical predictive model was examined by analysis of variance (ANOVA). The *P* value for the model lower than 0.05 (i.e., at 95 % confidence level) indicates that the model is considered to be statistically significant. The

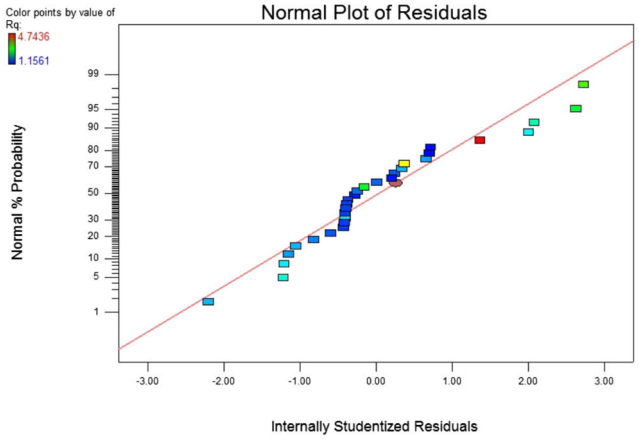

(a) Normal plot of residuals of SR

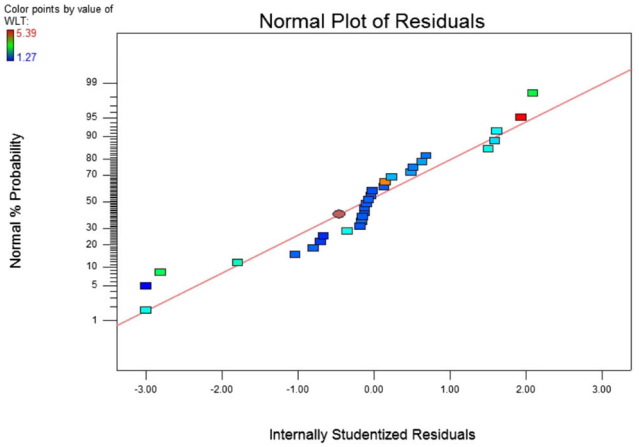

(b) Normal plot of residuals of WLT

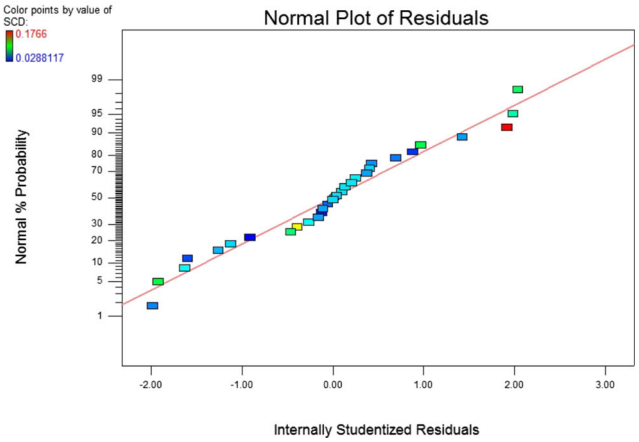

(c) Normal plot of residuals of SCD

Fig. 3 Normal plot of residuals of SR, WLT, and SCD

statistical analysis software, Design-Expert R 8.0, was applied in establishing the mathematical predicted models based on RSM. From the ANOVA Table 5 of SR (Rq), the P values of most of the terms for SR are less than 0.05, which means that these terms are significant to the predicted model. From the ANOVA Table 6 of WLT, it can be seen that the P values of most of the terms for WLT are less than 0.05, while from the ANOVA Table 7 of SCD, the similar results can be obtained that most of the terms for SCD are significant to its predicted model. Moreover, as shown in Tables 5, 6, and 7, R-Sq and R-Sq (adj) values of these models show the level of accuracy of the statistical model, which state that the models are acceptable with high level of confidence. Three mathematical predictive equations of SR, WLT, and SCD are, respectively, obtained as follows (1), (2), and (3). Figure 3a–c illustrates the normal probability plots of the residuals for SR, WLT and SCD. It is observed that the residuals of SR, WLT, and SCD are all located on a straight line, which means that the errors are normally distributed and the regression model is fairly reasonable and adequate. Mathematical regression models are regarded as input

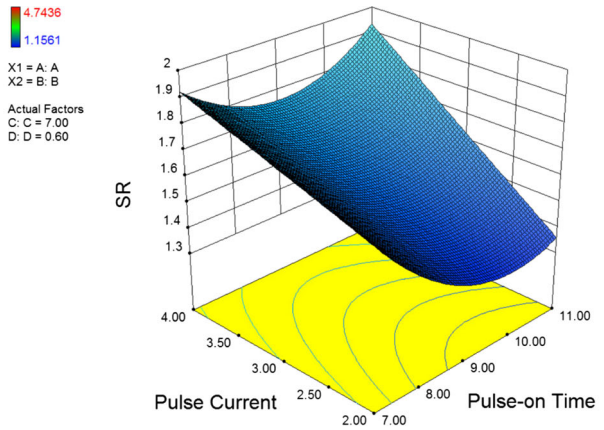

(a) SR versus pulse-on time & pulse current

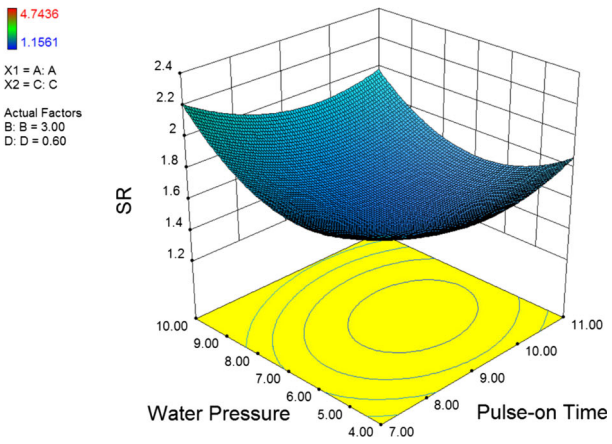

(b) SR versus pulse-on time & water pressure

Fig. 4 3D surface plots of SR versus different machining parameters

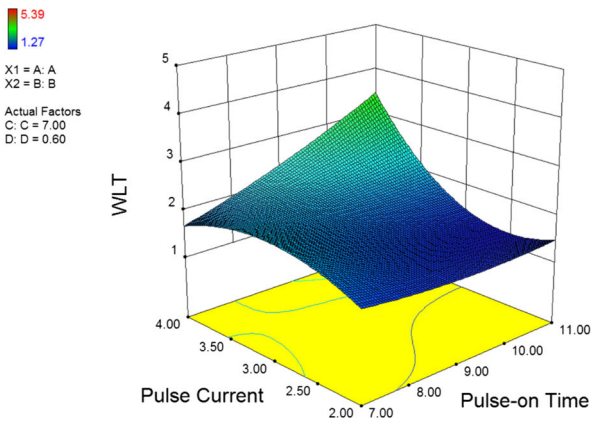

(a) WLT versus pulse-on time & pulse current

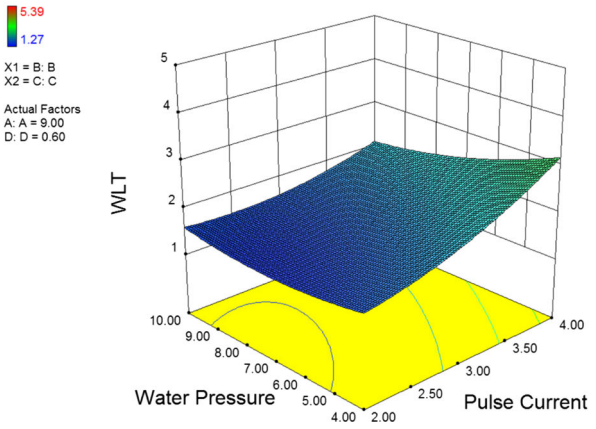

(b) WLT versus water pressure & pulse current

Fig. 5 3D surface plots of WLT versus different machining parameters

functions in NSGA-II, so the accuracy of these models play an important role in the performance of optimization.

$$\begin{aligned}\mathrm{Sq(Rq)} = {} & +20.76007 - 1.83563A - 5.58333B \\ & -2.72057C - 4.53557D + 0.36306A \times B \\ & +0.13211A \times C + 0.95942B \times C \\ & +2.74664B \times D + 1.24983C \times D \\ & +0.041517A^2 + 0.031370C^2 \\ & -0.045918A \times B \times C \\ & -0.70276B \times C \times D \end{aligned} \tag{1}$$

$$\begin{aligned}\mathrm{WLT} = {} & -7.29555 + 0.78130A + 12.68937B \\ & -1.40656C - 0.13750D - 1.44135A \times B \\ & +1.44135A \times C + 0.47318B \times C \\ & +0.030391A^2 - 2.93578B^2 + 0.021562C^2 \\ & -0.062240A \times B \times C + 0.35234A \times B^2 \end{aligned} \tag{2}$$

$$\begin{aligned}\mathrm{SCD} = {} & +0.38234 - 0.069457A - 0.14341B \\ & -0.011201C + 0.068428D + 0.021340A \times B \\ & +2.90553E - 003A \times C + 0.010562B \times C \\ & +1.53251E - 003A^2 - 1.76745E \\ & -003A \times B \times C \end{aligned} \tag{3}$$

3.2 Effect of variables on surface roughness

The 3D surface plots for SR variations against input parameters are shown in Fig. 4. It can be seen from Fig. 4a that the SR drops proportionally with the decrease of pulse current, while the SR goes down first and then goes up gradually as soon as the increase of pulse-on time. In Fig. 4b, it is observed that under the combined action of water pressure and pulse-on time, the minimum SR which means the optimal surface roughness can be obtained.

The main reason is that high pulse current leads to strong transient spark energy and electric field working on the specimens which damages the surface of workpiece. In short

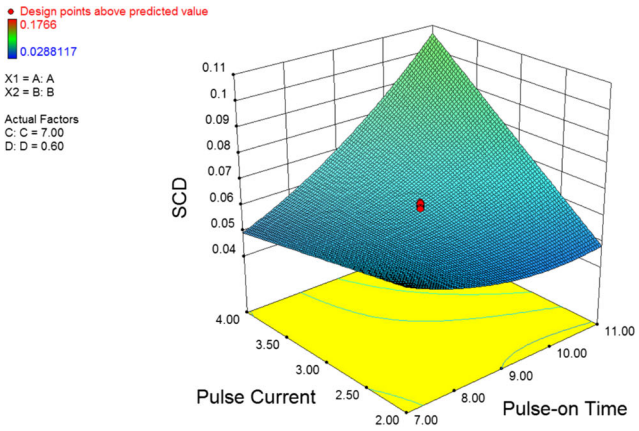

(a) SCD versus pulse-on time & pulse current

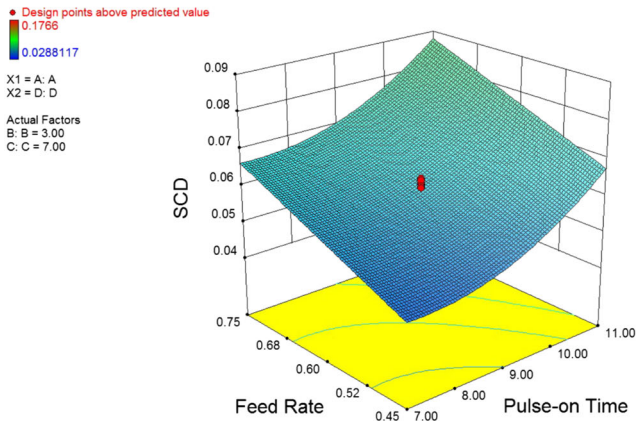

(b) SCD versus pulse-on time & offset

Fig. 6 3D surface plots of SCD versus different machining parameters

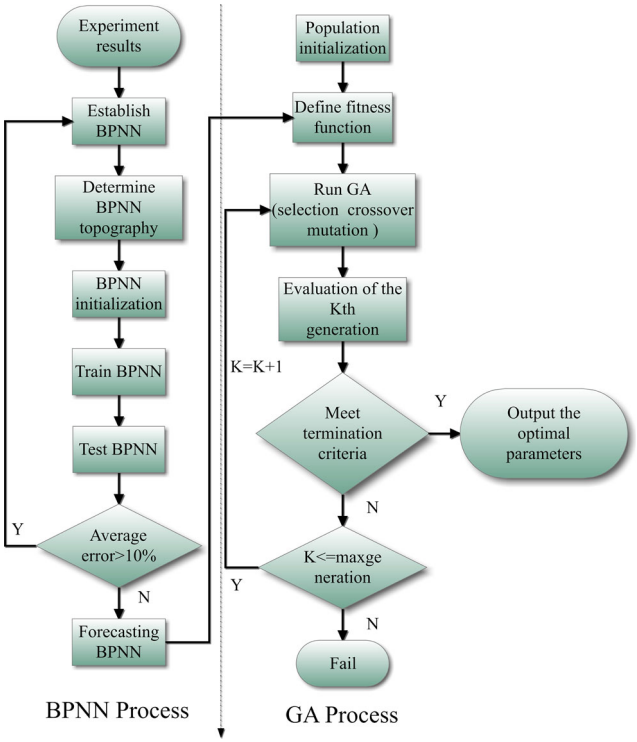

Fig. 7 Flow chart of the BPNN-GA

pulse-on time, there is not enough time to accumulate the thermal energy to melt and remove the materials. On the contrary, the too long pulse-on time results in excessive removal materials and damages the surface quality. Water pressure also plays a vital role in the performance of WEDM process because appropriate water pressure cannot only cool down the metallic materials but also wash away the metal debris from the wire tool and workpiece. But too much water pressure generates the vibration of wire tool which is harmful to the accuracy of WEDM process [16].

3.3 Effect of variables on white layer thickness

The 3D surface plots for WLT variations against input parameters are presented in Fig. 5. Figure 5a shows the complex influence of pulse-on time and pulse current on the WLT. When pulse current ranged from 3 to 4 A, with the decrease of pulse-on time, the WLT also declines dramatically. When pulse-on time set from 7 to 9μs, the WLT reaches the peak value at the nearby point of 3 A of pulse current. Oppositely, when pulse-on time set from 9 to 11μs, the bottom value of WLT comes out at the range from 3 to 2.5 A of pulse current. It can be concluded from Fig. 5b that pulse current rises, consequently the WLT soars up abruptly with the increase of water pressure. This phenomenon is attributed to the fact that an increase of pulse current and pulse-on time leads to an increase in the rate of thermal

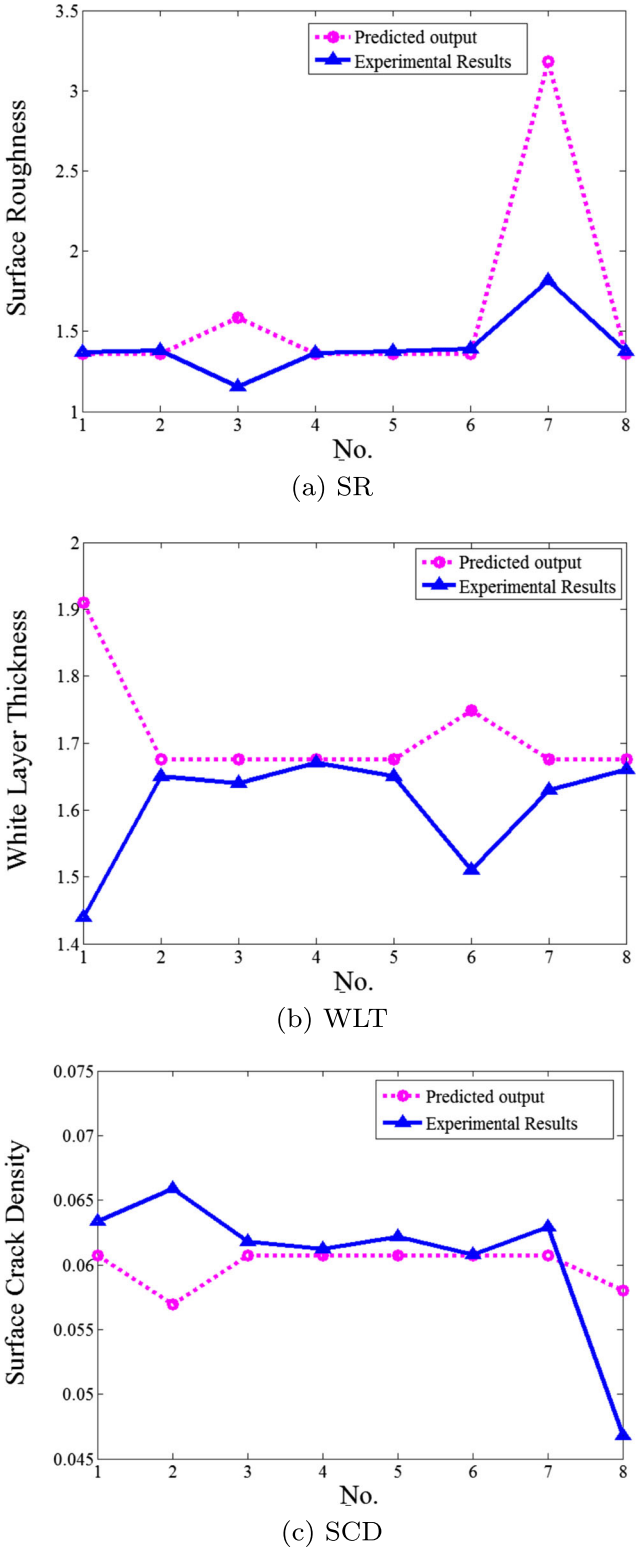

Fig. 8 Average errors between predicted results and experimental results for SR, WLT, and SCD

and electrical energy, which is subjected to both of the electrodes, and in the rate of melting and evaporation. Thus, the increasing heat is transferred into wire tool and workpiece

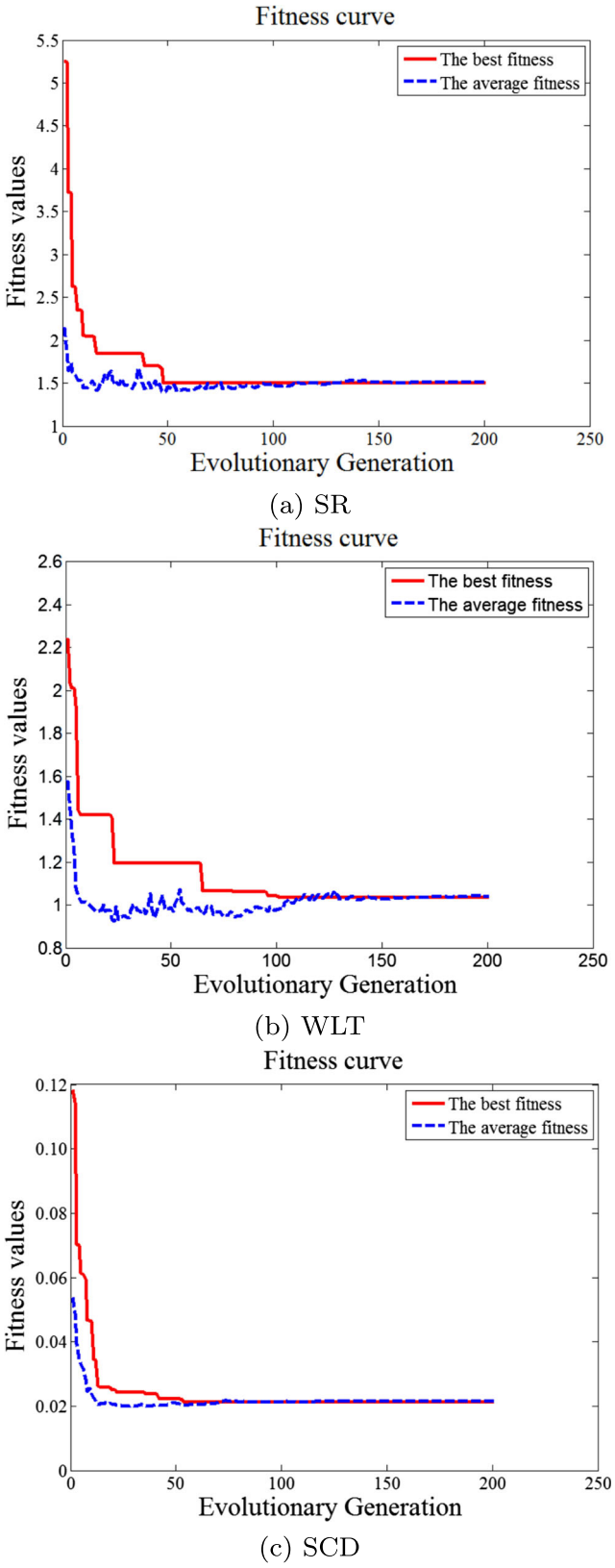

Fig. 9 Fitness curve of SR, WLT, and SCD

so that the dielectric begins to lose the ability of washing away and chilling the molten debris which accumulates and attaches to the surface of the parent materials. This remaining molten materials re-solidifies to form white layer and the thickness of white layer mainly depends on the volume of molten materials [17].

3.4 Effect of variables on surface crack density

The 3D surface plots for SCD variations against input parameters are presented in Fig. 6. It is observed in Fig. 6a that SCD ascends significantly as soon as pulse current or pulse-on time increases gradually. Figure 6b demonstrated a situation similar to Fig. 6a that is the increase of pulse current or offset leads to increasing the surface crack density. This is due to the combination of high pulse current, pulse-on time, and offset causing extreme thermal energy and stress which results in an increase in the dimension of the discharge crater, folds, inclusions, plastic deformation, residual stress, and the surface density cracks. Moreover, these residual stress, voids, and inclusions in the recast layer all have close relationship with forming the surface crack density.

4 Optimization of WEDM process

Two different methods, BPNN-GA and NSGA-II, were employed to optimize the WEDM process and obtain the optimal surface integrity. Single objective optimization using BPNN-GA was proposed to achieve the optimal solutions of SR, WLT, and SCD, respectively, while multi-objective optimization was implemented to obtain the optimal combination solutions of SR, WLT, and SCD simultaneously.

4.1 Optimized by BPNN-GA

Back propagation neural network (BPNN) is a multilayered feed-forward neural network. It has been widely used as an estimator to forecast WEDM performance. Genetic algorithm (GA) is a powerful archetype to solve optimizing problems in engineering. As the advantages in prediction and optimization mentioned above, it is becoming more and more efficient to couple BPNN with GA to deal with optimization problems. Thus, firstly, the experiment results were embed into BPNN to predict the performance under certain combination of process parameters. During the BPNN trained with 22 samples, the forecasting results were compared with the actual outputs. Then the error was backwards propagated through hidden layers and the weight of every network neuron was modified. After the network was constructed, the BPNN predicted outputs were

Table 8 Optimal combinations of parameters for the WEDM process

No.	A	B	C	D	SR (Rq)(μm)	WLT (μm)	SCD (μm/μm^2)
1	10.0	1.3	8.1	0.3	0.486	2.22	0.0222
2	11.6	4.5	12.9	0.8	0.534	3.07	0.0178
3	8.3	1.0	7.4	0.3	0.559	1.28	0.0322
4	8.0	1.0	7.2	0.3	0.630	0.98	0.0351
5	10.9	4.8	13.0	0.8	0.683	3.67	0.0141
6	7.5	1.0	7.1	0.3	0.771	0.74	0.0383
7	7.1	1.1	6.7	0.3	0.956	0.69	0.0357
8	11.3	4.9	12.9	0.7	1.227	2.23	0.0165
9	6.5	4.9	5.3	0.5	1.618	1.14	0.0270
10	6.2	4.8	6.0	0.5	2.072	0.72	0.0233

examined by the rest samples. When the error between the optimal results and the experimental results was acceptable, the GA was applied to optimize the parameters to achieve the desired performance. Before the beginning of GA, it first initialized the parent population, and the fitness was defined. Then it began to reproduce under certain probability of crossover and mutation. During the evolution process, units with higher fitness value were more likely to survive, while the other were obsoleted gradually. Finally, when the fittest solution meet the termination criteria, the optimal parameters were received (Fig. 7).

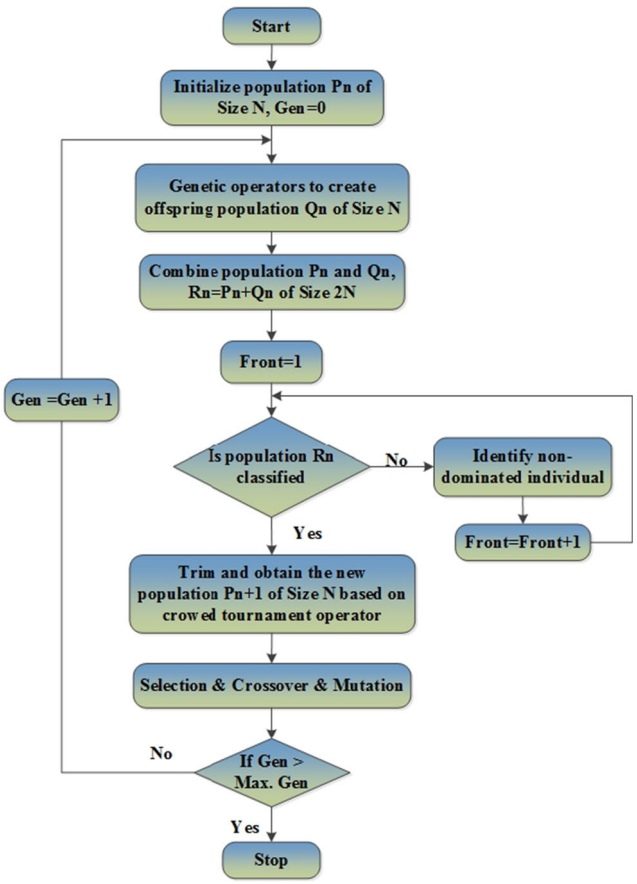

Fig. 10 Flow chart of NSGA-II

BPNN consists of many inter-connected artificial neurons often divided into three layers, namely input layers, hidden layers, and output layers. As the input and output layers are decided, which are 4 and 1, respectively, it is very important to determine the hidden layers to be accurate and effective. Several hidden layers were tested and it was found that the 4-6-5-1 topography was the most accurate network. Twenty-two samples were stochastically selected to train the BPNN and the rest (8 samples) was chosen to test the network. The test results as shown in Fig. 8 indicated that the average errors between predicted results and experimental results, which are 9.60, 5.90, and 6.02 % for SR, WLT, and SCD respectively, are absolutely acceptable due to all the errors below 10 %.

After the establishment of BPNN, the GA was employed for searching the optimal process parameters for the minimum SR, WLT, and SCD. GA is adopted real coding as individuals and the length of individual is four corresponding to four input parameters. The GA randomly generates an initial population by the roulette wheel method and the BPNN output results are set as fitness of GA. The fitness of GA is appropriate as well as the values of BPNN output are small, which achieves the high possibility to obtain the optimal solutions. In this section, the parameters of GA can be set as follows:

Population size = 40
Max generation = 700
Mutation probability = 0.01
Crossover probability = 0.9.

As the BPNN-GA cannot deal with more than one performance at a time, the optimization of surface integrity had to be done three times. Fitness values in Fig. 9 indicated the BPNN forecasting results. As Fig. 9 presents, there are both

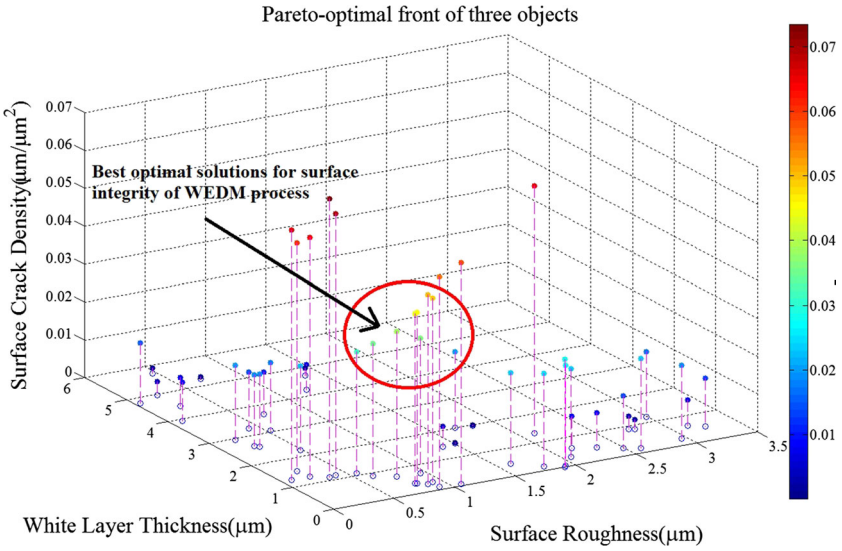

Fig. 11 Pareto-optimal front of three objectives

best fitness curve and average fitness curve for each performance. The optimal parameters for SR, WLT, and SCD, as well as the comparison between the predicted results and verified results under different situations, are listed in Table 8 and Table 9.

4.2 Optimized by NSGA-II

NSGA-II, which was proposed by Deb [18], conducts the elite-preserving and a phenotype crowd comparison operator to keep the diversity and reduce the computational complexity, therefore this evolutionary algorithm has an excellent competency in exploring the set of Pareto-optimal solutions to handle constrained multi-objective optimization problems. The general flow chart of the NSGA-II is shown in Fig. 10. This algorithm starts with the creation of a random parent population P_0 of size N, and them generates a children population Q_0 of size N by using genetic operators (including selection, crossover, mutation). New population R_0 of size 2N is formed by combining parents P_0 and offspring Q_0, and the random simplest mutation operator is applied randomly to create a solution from the entire search space R_0. The solutions are classified into various non-dominated fronts, which are ranked based on their non-dominance level. The crowded tournament selection operator is applied to select the better solution and trim the population to form the new generation P_1 according to the two rules: (1) a non-dominated front in the population and (2) a local large crowding distance.

The mathematical predicting models for SR, WLT, and SCD are optimized by using NSGA-II which has the capacity of improving the primary goals of minimum SR, minimum WLT and minimum SCD simultaneously. The objectives and optimization model are presented as follows:

Objective 1 = SR
Objective 2 = WLT
Objective 3 = SCD
Min f(x) = SR, WLT, SCD

The mathematical models are put into the three objectives optimization, and thereafter the following parameters were listed based on the study to get optimal solutions with high efficiency and accuracy:

1. Population size = 50
2. Maximum number of generations = 200
3. Mutation probability = 0.2
4. Crossover probability = 0.7

Pareto-optimal front of three-objective optimization and the best optimal solutions for WEDM machining (in the red circle) which balances the performance of SR, WLT, and SCD are both shown in Fig. 11. It is observed clearly that the whole optimal solutions are no bias towards too high side or too low side, and none of them is absolutely better than any other, which is attributed to NSGA-II allowing the all non-dominated fronts to coexist in the population. Moreover, though the high surface quality needs the SR, WLT, and SCD all keep on a low level, if the few surface cracks (SCD) is much required, the white layer thickness

Table 9 Results of the experimental confirmation about BPNN-GA optimization

Output	Optimal parameters						
	A	B	C	D	Pre.	Exp.	Relative error (%)
SR	8.09	2.05	2.42	0.55	1.505	1.225	18.60 %
WLT	9.08	3.29	6.79	0.78	1.04	1.17	12.50 %
SCD	8.76	2.24	4.36	0.39	0.0212	0.0204	3.77 %

Table 10 Results of the experimental confirmation about NSGA-II optimization

No.	Optimal parameters				SR			WLT			SCD		
	A	B	C	D	Pre.	Exp.	Relative error (%)	Pre.	Exp.	Relative error (%)	Pre.	Exp.	Relative error (%)
8	11.3	4.9	12.9	0.7	1.227	1.357	10.59 %	2.23	2.52	13.00 %	0.0165	0.0211	27.88 %
9	6.5	4.9	5.3	0.5	1.618	1.807	11.68 %	1.14	1.45	27.19 %	0.0270	0.0317	17.40 %

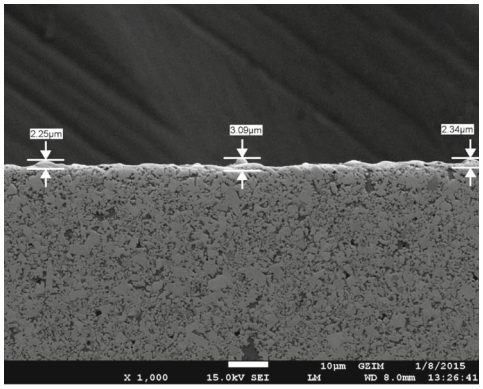

(a) SEM images about White layer of No.21 in Table 4 before optimization

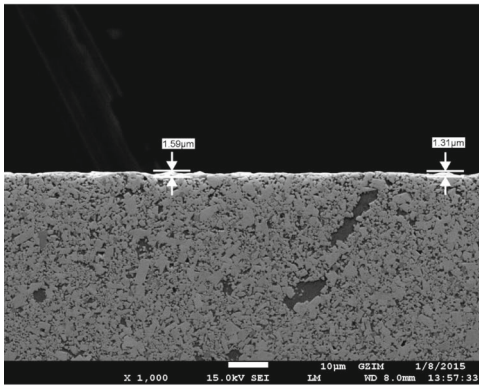

(b) SEM images about White layer of No.9 in Table 8 using NSGA-II optimization

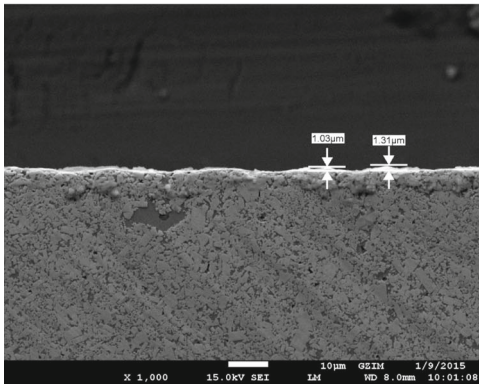

(c) SEM images about White layer of WLT in Table 9 using BPNN-GA optimization

Fig. 12 SEM images about White layer of several WEDM specimens

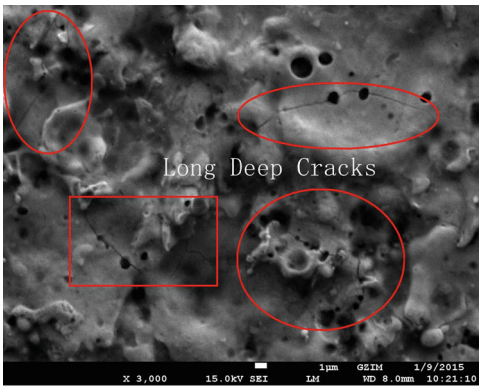

(a) SEM images about surface crack of No.29 in Table 4 before optimization

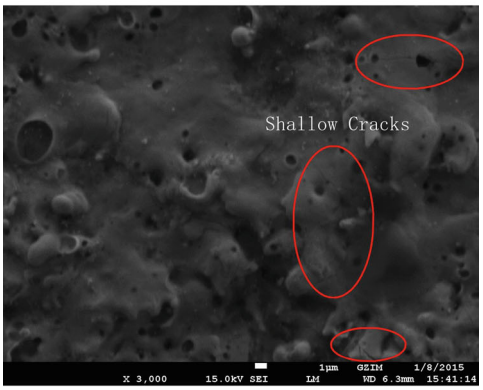

(b) SEM images about surface crack of No.8 in Table 8 using NSGA-II optimization

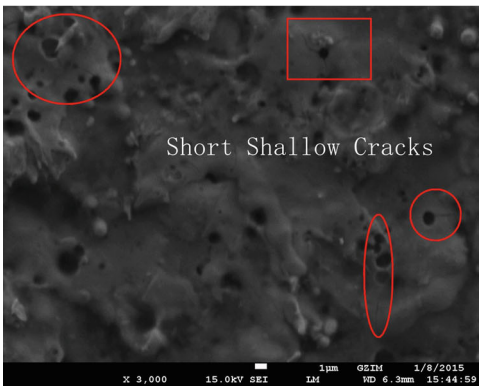

(c) SEM images about surface crack of SCD in Table 9 using BPNN-GA optimization

Fig. 13 SEM images about surface crack of several WEDM specimens

and surface roughness should make a compromise. Considering the actual requirements of machining, as shown in Table 8, ten better Pareto-optimal solutions are obtained at the end of NSGA-II operation due to the whole optimal set that includes some impractical solutions.

4.3 Analysis of the optimal results and verification

Two different approaches, BPNN-GA and NSGA-II, were employed to optimize surface integrity and obtain optimal combination of process parameters for SR, WLT, and SCD, respectively. Confirmation experiments should be conducted to verify the accuracy of the optimal solutions and judge which optimization method is more effective and significant, and then to find out the effective optimal set under the different process condition to guide the actual machining. The results of confirmation experiments under the optimal combination of process parameters from the two methods are listed in Tables 9 and 10. Before confirmation experiments, based on approximation method, these optimal combinations of process parameters were slightly adjusted into the appropriate values which can be obtained according to the characteristics of WEDM. Three times the same confirmation experiment has been repeated and the mean results have been recorded which contrast with the corresponding optimal solutions. As shown in Table 9, the relative errors of SR, WLT, and SCD from BPNN-GA are 18.6, 12.5, and 3.77 %, respectively, which mean that this method is effective and acceptable due to all the relative errors within 20 %. As presented in Table 10, the relative errors of Pareto-optimal solutions (nos. 8 and 9) from NSGA-II are all at an acceptable and reasonable level, not more than 30 %. It can be seen obviously that two optimization methods have advantages and disadvantages. As for BPNN-GA, it has a higher predicted accuracy of surface integrity characteristics (SR, WLT, and SCD), respectively, but it cannot balance the three characteristics at the same time. On the other hand, though NSGA-II sacrifice some predicted accuracy, this method can provide the optimal solutions considering the conditions of three characteristics simultaneously. Therefore, the most appropriate optimal combinations of process parameters from the different optimization methods can be chosen according to the actual machine conditions and requirements. For instance, if the long fatigue life of workpiece is desired, the process parameter combination which can obtain the minimum SCD should be selected because the surface crack has a close relation to the fatigue life. Similarly, the much clean surface requires the process parameter combination which can obtain the minimum SR and WLT. Figures 12 and 13 demonstrate that two-dimensional SEM images about white layer and surface crack of several WEDM specimens before optimization and after optimization. It is observed apparently that at the same level of surface roughness, compared with the original experimental results, white layer thickness and surface crack density of several WEDM specimens has been decreased after parameter optimization, thus the quality of surface integrity has been improved after optimization using NSGA-II and BPNN-GA.

5 Conclusion

In this paper, based on RSM, BPNN-GA, and NSGA-II methods, the investigation about the effect and optimization of process parameters, which are pulse-on time, pulse current, water pressure and feed rate, on surface integrity of workpiece including SR, WLT, and SCD in WEDM processing tungsten tool YG15 was conducted. The following conclusions are drawn from the present research.

1. After the analysis of variance and interaction of process parameter, the results manifest that the pulse-on time and pulse current have a significant effect on the SR, WLT, and SCD, while water pressure and feed rate also have a close relationship with surface integrity but are not the most important factors affecting the surface integrity.
2. The single objective optimization method by BPNN-GA and multi-objective optimization method by NSGA-II were proposed to optimize the surface integrity of workpiece in WEDM and obtain a set of appropriate process parameter combinations. Thus, the most suitable process parameter combinations can be selected according to the actual machine conditions and requirements, which can help increase the surface quality and precision of WEDM process and reduce defective rate for industrial application.

Acknowledgments This research is supported by the China Scholarship Council and the National Natural Science Foundation of China (NSFC) under Grant No. 51175207.

References

1. Newton TR, Melkote SN, Watkins TR, Trejo RM, Reister L (2009) Investigation of the effect of process parameters on the formation and characteristics of recast layer in wire-edm of inconel 718. Mater Sci Eng A-Struct 513:208–215
2. Qu J, Scattergood RO, Shih AJ (2002) Development of the cylindrical wire electrical discharge machining process, part 2: surface integrity and roundness. J Manuf Sci Eng 124(3):708–714
3. Velterop L (2003) Influence of wire electrical discharge machining on the fatigue properties of high strength stainless steel. Mater Sci Forum 426-432:1017–1022
4. Caydas U, Ahmet H (2007) Modeling and analysis of electrode wear and white layer thickness in die-sinking edm process through

response surface methodology. Int J Adv Manuf Technol 38(11-12):1148–1156
5. Yildiz Y, Sundaram MM, Rajurkar KP (2013) Empirical modeling of the white layer thickness formed in electrodischarge drilling of berylliumCcopper alloys. Int J Adv Manuf Technol 66(9-12):1745–1755
6. Pradhan MK (2013) Estimating the effect of process parameters on surface integrity of edmed aisi d2 tool steel by response surface methodology coupled with grey relational analysis. Int J Adv Manuf Technol 67(9-12):2051–2062
7. Lee HT, Tai TY (2003) Relationship between edm parameters and surface crack formation. J Mater Process Technol 142(3):676–683
8. Puri AB, Bhattacharyya B (2005) Modeling and analysis of white layer depth in a wire-cut edm process through response surface methodology. Int J Adv Manuf Technol 25(3-4):301–307
9. Shahali H, Yazdi MRS, Mohammadi A, Iimanian E (2012) Optimization of surface roughness and thickness of white layer in wire electrical discharge machining of din 1.4542 stainless steel using micro-genetic algorithm and signal to noise ratio techniques. Proc IME B J Eng Manuf 226(5):803–812
10. Shabgard M, Oliaei SNB, Seyedzavvar M, Najadebrahimi A (2011) Experimental investigation and 3d finite element prediction of the white layer thickness, heat affected zone, and surface roughness in edm process. J Mech Sci Technol 25(12):3173–3183
11. Zhang G, Zhang Z, Ming W, Guo J, Huang Y, Shao X (2014) The multi-objective optimization of medium-speed wedm process parameters for machining skd11 steel by the hybrid method of rsm and nsga-ii. Int J Adv Manuf Technol 70(9-12):2097–2109
12. Ming W, Zhang Z, Zhang G, Huang Y, Guo J, Chen Y (2014) Multi-objective optimization of 3d-surface topography of machining yg15 in wedm. Mater Manuf Processes 29(5):514–525
13. Zhang G, Zhang Z, Guo J, Ming W, Li M, Huang Y (2013) Modeling and optimization of medium-speed wedm process parameters for machining skd11. Mater Manuf Processes 28(10):1124–1132
14. Rong Y, Zhang Z, Zhang G, Yue C, Gu Y, Huang Y, Wang C, Shao X (2015) Parameters optimization of laser brazing in crimping butt using taguchi and bpnn-ga. Opt Lasers Eng 67:94–104
15. Montgomery DC (2001) Design and analysis of experiments. Wiley, Hoboken
16. Zhang G, Chen Z, Zhang Z, Huang Y, Ming W, Li H (2014) A macroscopic mechanical model of wire electrode deflection considering temperature increment in ms-wedm process. Int J Mach Tools Manuf 78:41–53
17. Bhattacharyya B, Gangopadhyay S, Sarkar BR (2007) Modelling and analysis of edmed job surface integrity. J Mater Process Technol 189(1):169–177
18. Deb K, Pratap A, Agarwal S, Meyarivan T (2002) A fast and elitist multiobjective genetic algorithm: NSGA-II. IEEE T Evolut Comput 6:182–197